Chapter 1

α-Synuclein: Background, Methods, and Initial Studies

1.1 INTRODUCTION

α-Synuclein.

Parkinson's disease develops from the loss of dopaminergic neurons in the *substania nigra* region located in the brain stem. It also can be characterized by the presence of intracellular inclusions, namely Lewy bodies,[1] which are mostly comprised of α-synuclein (α-syn).[2,3] Although the detailed role of α-syn in the pathogenic mechanism is unclear, the protein is commonly found in the cytosol and presynaptic nerve terminals of a neuron.[4-6] The localization mechanism of α-syn is not well understood. Unlike other presynaptic proteins, α-syn does not tightly associate with the synaptic plasma membrane or the synaptic vesicle.[7,8]

Though the protein is characterized to be unstructured *in vitro,*[9] numerous experimental data now indicate that α-syn is not a random coil, but contains regions of structural preferences.[10-15] In the presence of acidic phospholipid vesicles, the protein will adopt α-helical structures. Notably, α-syn does not appear to interact with neutral phospholipid vesicles.[16] These structures have been characterized by circular dichroism (CD),[17] nuclear magnetic resonance (NMR),[18-20] and electron paramagnetic resonance (EPR) spectroscopies.[21,22] These conformers are particularly important because α-helical dimers and multimers have been observed in lipid environments.[23,24] Furthermore, there is evidence suggesting that these oligomers may participate in membrane permeabilization, one of the proposed molecular pathways of disease.[25,26]

The primary amino acid sequence of human α-syn has been illustrated in **Figure 1.1**. The N-terminal region of α-syn includes seven imperfect repeats (consensus XKTKEGVXXXX) containing eleven amino acids each.[4] This repeating pattern is commonly found in exchangeable apolipoproteins, implying that α-syn has the capability of binding to lipid surfaces reversibly.[17,27-29] The C-terminal tail is rich in glutamate, whose acidic properties prevent tail association with the negatively-charged phospholipid membrane. Another particularly interesting region is the non-amyloid β component (NAC) domain located between residues 61 and 95. This peptide fragment is highly hydrophobic and has been identified in senile plaques characteristic of Alzheimer's disease.[30]

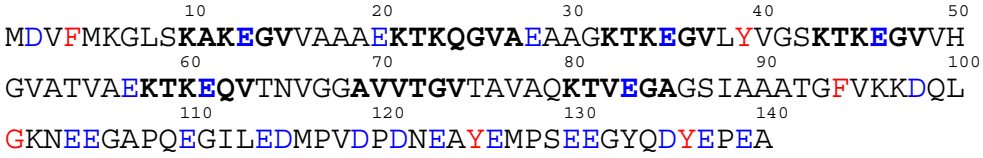

Figure 1.1. Amino acid sequence for α-syn. The acidic residues (blue) and Trp mutation sites (red) are highlighted. The seven imperfect repeats are bolded.

1.2 MATERIALS AND METHODS

Materials.

Lipids were purchased in chloroform from Avanti Polar Lipids (Alabaster, AL). N-acetyl-tryptophanamide (NATA), sodium dodecyl sulfate (SDS), and tetranitromethane (TNM) were used as received from Sigma. BL21(DE3)pLysS was obtained from Stratagene.

Protein Preparation, Modification, and Characterization.

M. Goedert (Medical Council Research Laboratory of Molecular Biology, Cambridge, U.K.) provided the wild-type human α-syn expression vector.[8] Mutations were introduced in three various positions by site-directed mutagenesis. All the sequences were confirmed by DNA sequencing.

Expression and purification of mutants were achieved following previously published protocols with minor modifications.[31] The mutant plasmids were transformed into *E. coli* BL21(DE3)pLysS and plated onto LB agar plates containing 34 μg/mL of chloramphenicol and 100 μg/mL of ampicillin. Single colonies were chosen and grown in 25 mL of LB medium with the same antibiotic concentrations for 15 hours. Cells harvested from this starter culture were used to inoculate large LB medium with the same antibiotic concentrations. Cells were grown in 4 L flasks containing 1 L of medium at 30 °C until $Abs_{600} \sim 0.6$. IPTG was then added and the cells were harvested 6 hours after induction. The harvested cells were stored at -80 °C.

α-Syn was extracted from the frozen cells by boiling and acid precipitation. The crude protein solution was then purified by Q-Sepharose Fast Flow 16/10 column (Amersham Biosciences) by fast protein liquid chromatography (FPLC) equilibrated with 20 mM Tris buffer (pH 8.0). The protein was eluted with a gradient from 0 to 0.5 M NaCl. The semi-pure protein fractions were combined and further purified on a Mono-Q 10/10 column (Amersham Biosciences).

Proteins were nitrated following published protocol with minor modification.[32] Purified and concentrated (~100 μM) α-syn in 20 mM Tris buffer with 200-300 mM NaCl at pH 8.0 was stirred under Ar for 20 min in the dark. To the stirring protein solution (850 μL), TNM in ethanol [1% (vol/vol), 75 μL] was added dropwise. A second aliquot of TNM solution was added after 10 min. After another 10 min, the reaction was desalted by gel filtration chromatography (HiPrep Desalting 26/10, Amersham Biosciences) using FPLC. The desalted protein was then purified on a Mono-Q 10/10 column.

The concentration of non-nitrated protein was determined using a molar extinction coefficient estimated by amino acid content: ε_{280} = 6 970 $M^{-1} \cdot cm^{-1}$, while nitrated protein concentration was determined by literature molar extinction coefficient: ε_{381} = 2 200 $M^{-1} \cdot cm^{-1}$.[33] Absorption measurements were carried out by a Hewlett-Packard 8452 diode array spectrophotometer. Purities of all protein samples were evaluated by SDS-PAGE on a Pharmacia PhastSystem (Amersham Biosciences). Molecular weights of all protein samples were determined by electrospray mass spectrometry (California Institute of Technology Protein/Peptide Microanalytical

Laboratory). All protein stock solutions were concentrated using Amicon YM-3 (molecular weight cutoff 3 kD; Millipore) and stored in -80 °C.

Preparation of Membrane Mimics.

Small Unilammelar Vesicles (SUVs) were made from published protocols.[34] Chloroform from the lipid solutions was removed under a stream of Ar and then dried under vacuum. 20 mM sodium phosphate (NaP_i) buffer (pH 7.4) was used to resuspend the dried lipid into a concentration of 5 mg/mL. The lipid solution was then sonicated by a Branson ultrasonicator microtip (Plainview, NJ) for 30 min at 50% duty cycle (200 W). The sonicated SUVs were then diluted to a final concentration of 2 mg/mL with NaP_i buffer and equilibrated overnight at room temperature. Titanium dust and particulates were removed by centrifuging the SUV solution at 10,000 × *g* for 10 min. Freshly prepared SUVs were used for all experiments. SDS micelles were made by preparing a 40 mM solution of SDS. The micelle solution was then filtered by 0.22 μm filter before use.

Steady-State Measurements.

Tryptophan (Trp) luminscence spectra were obtained by exciting the sample at 295 nm (1 nm band-pass) and recording between 300 and 500 nm (1 nm band-pass, 0.25 s integration) on a Fluorolog2 spectrofluorimeter (Jobin Yvon, Longjumeau, France) in a 1 cm cuvette. For kinetics studies, the sample was excited at 290 nm (1 nm band pass) and the fluorescence emission was monitored at 350 nm (4 nm band-pass, 0.5 s integration). Circular dichroism spectra were measured by Aviv 62ADS

spectropolarimeter (Aviv Associates, Lakewood, NJ) in a 1 mm cuvette at 25 °C. Measurements of 5 μM α-synuclein were recorded between 200 nm and 260 nm with a band-pass of 1.5 nm.

Time-Resolved Fluorescence Measurements.

Trp fluorescence-decay kinetics were measured as described in literature.[35] The experimental samples were prepared as described above and deoxygenated by 30 cycles of evacuation/Ar-fill on a Schlenk line. The Trp was excited by a 292 nm polarized pulse (35° from vertical) from a regeneratively amplified femtosecond Ti:sapphire laser (Spectra-Physics). Interference filters were used to select Trp emissions between 325 and 400 nm. The Trp fluorescence decay kinetics were recorded in single photon counting mode by a picosecond streak camera (Hamamatsu Photonics C5680, Hamamatsu City, Japan). Control experiments were performed using the Trp model complex, NATA.

Data Analysis.

Trp fluorescence decay kinetics were modeled with **Equation 1**, where $I_0(t)$ is the Trp fluorescent decay without the presence of quencher, $P(r)$ is the probability of observing the donor-acceptor distance r, and $k_{et}(r)$ is the energy transfer rate at distance r.

$$I(t) = I_0(t)\int P(r)\exp(-k_{et}(r)t)dr \quad (1)$$

The decay kinetics were fitted to extract the distance distributions by numerical inversion of the Laplace transform describing $I(t)$. This inversion was

constrained by the requirement of $P(r) \geq 0$. The narrowest $P(k)$ distributions were projected by a linear least-squares (LLS) MATLAB (Mathworks, Natick, MA) algorithm with a non-negative constraint (LSQNONNEG). The $P(k)$ distribution obtained from the above fitting routine was recasted into a distribution of r using the Förster equation (**Equation 2**), where k_R is the measured radiative decay rate constant of excited NATA.

$$r = R_0(\Phi_D k_R / k_{et})^{1/6} \quad (2)$$

1.3 RESULTS AND DISCUSSION

Different SUVs studies.

Five types of lipids have been utilized in this thesis (**Figure 1.2**). Previous work has suggested that α-syn will only form a helical structure when acidic SUVs are present. Therefore, most of the SUVs were made of a 1:1 molar mixture of 1-palmitoyl-2-oleoyl-*sn*-glycero-3-phosphocholine (POPC) and 1-palmitoyl-2-oleoyl-*sn*-glycero-3-phosphate (POPA). The other three types of lipids used were 1-palmitoyl-2-stearoyl(6,7-dibromo)-*sn*-glycero-3-phosphocholine (6,7-DiBr), 1-palmitoyl-2-stearoyl(11,12-dibromo)-*sn*-glycero-3-phosphocholine (11,12-DiBr), and N-dinitrophenyl phosphatidylethanolamine (DNP).

We have prepared some SUVs with only POPC lipids, which are not charged. **Figure 1.3** shows the CD spectrum of wild type α-syn in solution (red), SDS micelles (blue) , 1:1 POPC:POPA SUVs (black), and POPC (green) SUVs. The α-helical signature peaks were demonstrated when wild type α-syn was mixed with 1:1

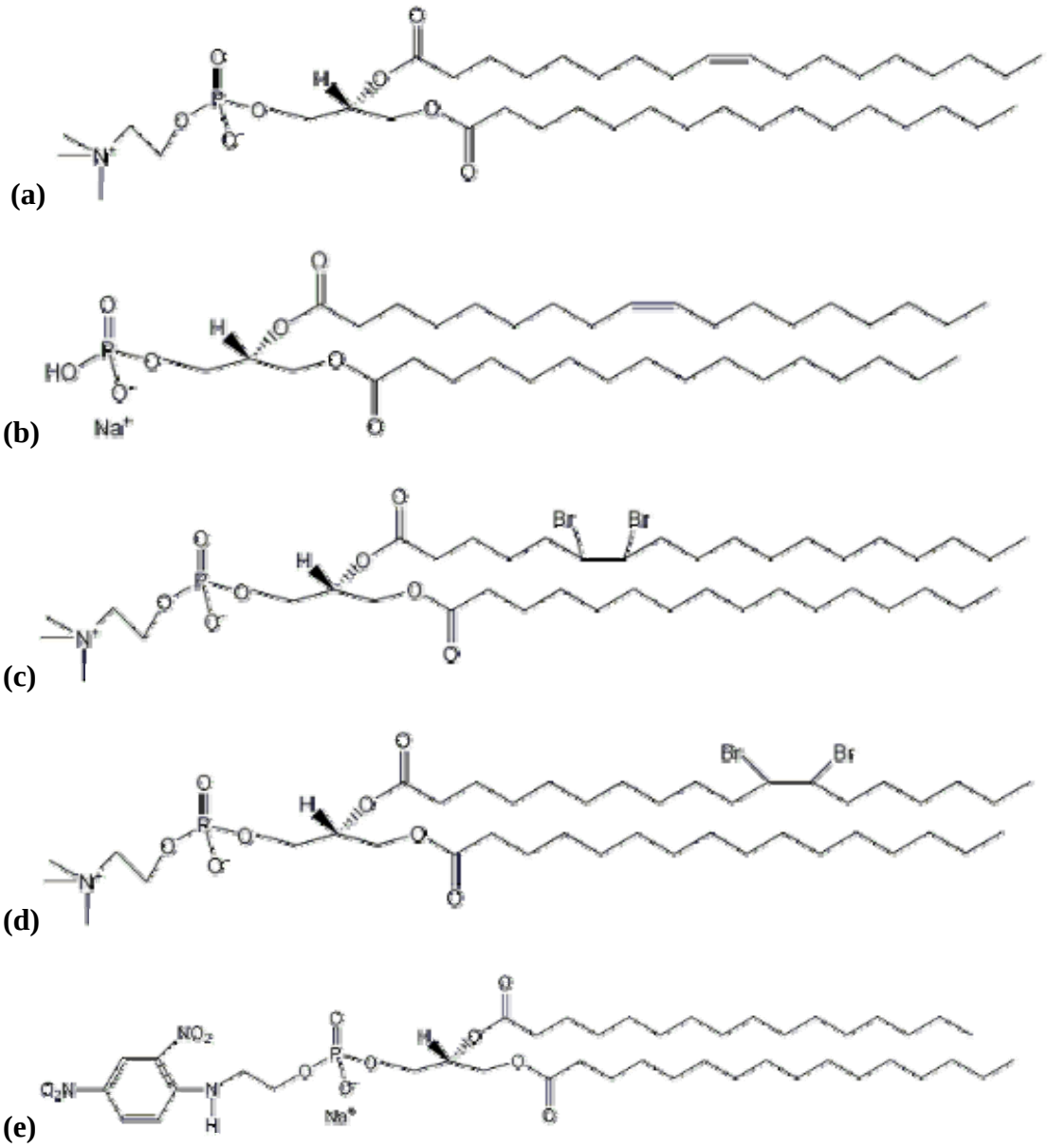

Figure 1.2. Structure of **(a)** 1-palmitoyl-2-oleoyl-*sn*-glycero-3-phosphocholine (POPC), **(b)** 1-palmitoyl-2-oleoyl-*sn*-glycero-3-phosphate (POPA), **(c)** 1-palmitoyl-2-stearoyl(6,7-dibromo)-*sn*-glycero-3-phosphocholine (6,7-DiBr), **(d)** 1-palmitoyl-2-stearoyl(11,12-dibromo)-*sn*-glycero-3-phosphocholine (11,12-DiBr), and **(e)**N-dinitrophenyl phosphatidylethanolamine (DNP)

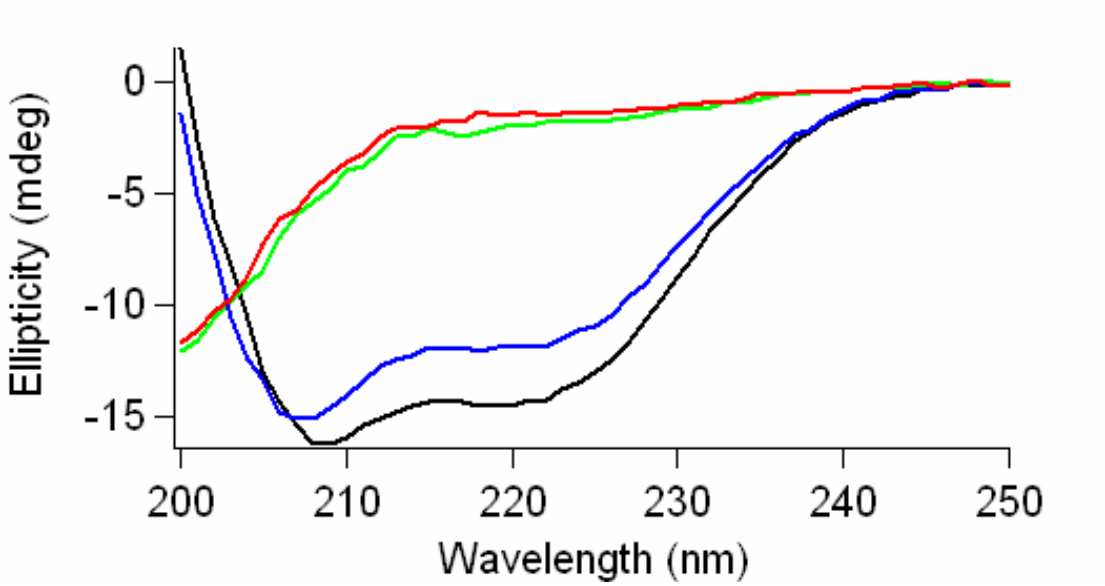

Figure 1.3. The CD signal for wild-type α-syn in 20 mM NaP_i buffer (red), 31 mM SDS micelles (blue), POPC SUVs (green), and 1:1 POPC:POPA SUVs (black)

POPC:POPA SUVs and SDS micelles. However, the CD spectra are comparable in solution and POPC SUVs, implying that minimal structures were induced when neutral vesicles are utilized.

This phenomenon was further proven by submitting a Trp-containing α-syn mutant (W39/Y55) to steady-state fluorescence spectroscopy in the aforementioned environments (**Figure 1.4**). Protein local environments can often be elucidated from Trp emissions.[36-39] The data suggests the λ_{max} of Trp emission for this α-syn mutant in solution is 347 nm. This emission maxima is similar when the mutant was placed in POPC SUVs (λ_{max} = 348 nm).

On the contrary, blue-shifted emission was observed when the α-syn mutant was placed in 31 mM SDS micelles (λ_{max} = 336 nm). This blue-shifted emission implies that the Trp is in a more hydroprobic environment, namely the micelles. In addition, an even more pronounced blue-shifted emission was observed when the mutant was placed in 1:1 POPC:POPA SUVs (λ_{max} = 332 nm). These CD and steady-state fluorescence studies show that the acidic lipids must be incorporated into the SUVs in order to induce structural formation of α-syn.

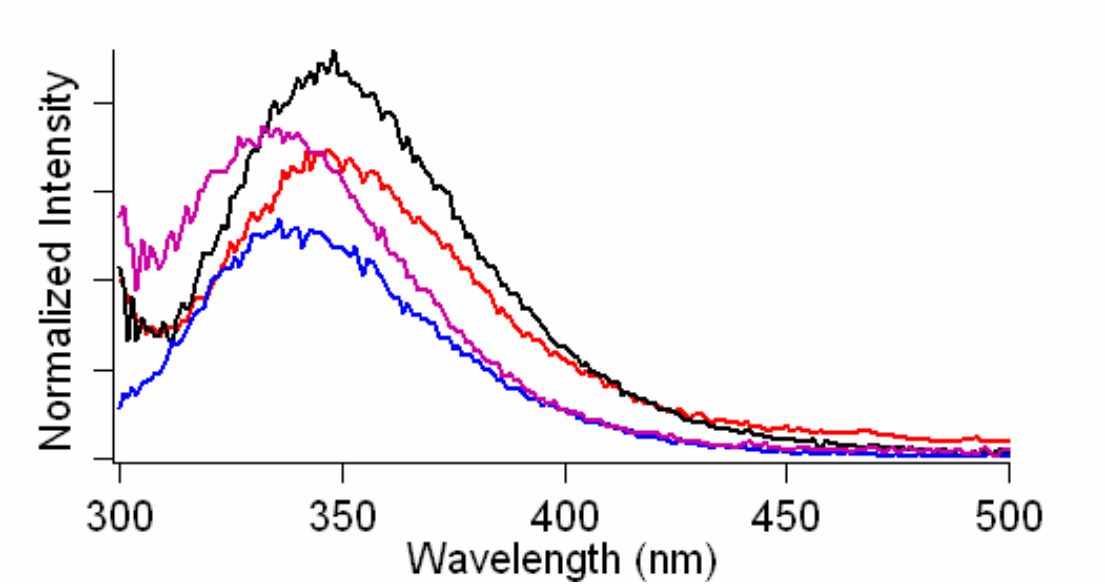

Figure 1.4. The steady-state fluorescence spectra of W39/Y55 α-syn mutants in the presence of 20 mM NaPi buffer (red), 31 mM SDS micelles (blue), POPC SUVs (black), and 1:1 POPC:POPA (purple)

α-Syn Insertion Studies.

It is important to determine the timescale for α-syn insertion into the bilayer to ensure that spectroscopic studies will be carried out after the samples have been fully equilibrated. As mentioned above, the quantum yield of Trp increases when it is placed in a more hydrophobic environment. We took advantage of this phenomenon to study the insertion kinetics of α-syn. The emission was monitored in 350 nm. Therefore, when the Trp is inserted into the bilayer, the fluorescence will increase significantly.

Figure 1.5 shows the fluorescence spectra when W4 was mixed with 1:1 POPC:POPA SUVs. A concentrated W4 solution was injected into a cuvette of SUVs when time = 62 s. Therefore, a significant increase of emission was observed at that point. After the sharp increase, there was a step of an appreciable decrease of fluorescence that lasts approximately another 150 s (inset). This implies that the insertion of α-syn into the lipid bilayer is almost instantaneous, followed by an equilibration step that lasts for minutes.

Trp's emission was further monitored for another 1.5 h, during which a very slow decrease of fluorescence intensity was observed. This event can be attributed to photodamage caused by long irradiation of the Trp.

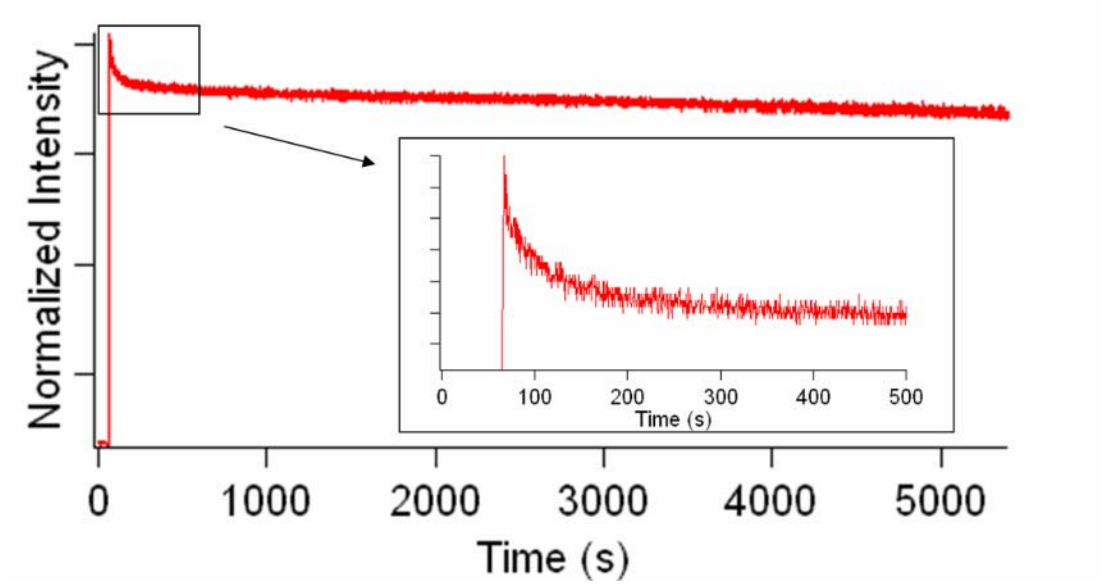

Figure 1.5. Steady-state fluorescence of Trp4 inserting into 1:1 POPC:POPA SUVs monitored at 350 nm

1.4 ACKNOWLEDGEMENT

This work is completed in collaboration with Dr. Jennifer C. Lee.

1.5 REFERENCE

(1) Galvin, J. E.; Lee, V. M.; Schmidt, M. L.; Tu, P. H.; Iwatsubo, T.; Trojanowski, J. Q..*Adv. Neurol.* **1999**, *808*, 313–324.
(2) Spillantini, M. G.; Crowther, R. A.; Jakes, R.; Hasegawa, M.; Goedert, M. *Proc. Natl. Acad. Sci. U. S. A.* **1998**, *95*, 6469–6473.
(3) Spillantini, M. G.; Schmidt, M. L.; Lee, V. M. Y.; Trojanowski, J. Q.; Jakes, R.; Goedert, M. *Nature* **1997**, *388*, 839–840.
(4) George, J. M.; Jin, H.; Woods, W. S.; Clayton, D. F. *Neuron* **1995**, *15*, 361–372.
(5) Iwai, A.; Masliah, E.; Yoshimoto, M.; Ge, N. F.; Flanagan, L.; Desilva, H. A. R.; Kittel, A.; Saitoh, T. *Neuron* **1995**, *14*, 467–475.
(6) Irizarry, M. C.; Growdon, W.; Gomez-Isla, T.; Newell, K.; George, J. M.; Clayton, D. F.; Hyman, B. T. *J. Neuropath. Exp. Neur.* **1998**, *57*, 334–337.
(7) Maroteaux, L.; Scheller, R. H. *Mol. Brain Res.* **1991**, *11*, 335–343.
(8) Jakes, R.; Spillantini, M. G.; Goedert, M. *Febs. Lett.* **1994**, *345*, 27–32.
(9) Weinreb, P. H.; Zhen, W. G.; Poon, A. W.; Conway, K. A.; Lansbury, P. T. *Biochemistry* **1996**, *35*, 13709–13715.
(10) Bertoncini, C. W.; Jung, Y. S.; Fernandez, C. O.; Hoyer, W.; Griesinger, C.; Jovin, T. M.; Zweckstetter, M. *Proc. Natl. Acad. Sci. U. S. A.* **2005**, *102*, 1430–1435.
(11) Lee, J. C.; Gray, H. B.; Winkler, J. R. *J. Am. Chem. Soc.* **2005**, *127*, 16388–16389.
(12) Lee, J. C.; Langen, R.; Hummel, P. A.; Gray, H. B.; Winkler, J. R. *Proc. Natl. Acad. Sci. U. S. A.* **2004**, *101*, 16466–16471.
(13) Lee, J. C.; Lai, B. T.; Kozak, J. J.; Gray, H. B.; Winkler, J. R. *J. Phys. Chem. B* **2007**, *111*, 2107–2112.
(14) Dedmon, M. M.; Lindorff-Larsen, K.; Christodoulou, J.; Vendruscolo, M.; Dobson, C. M. *J. Am. Chem. Soc.* **2005**, *127*, 476–477.
(15) Bernado, P.; Bertoncini, C. W.; Griesinger, C.; Zweckstetter, M.; Blackledge, M. *J. Am. Chem. Soc.* **2005**, *127*, 17968–17969.
(16) Conway, K. A.; Harper, J. D.; Lansbury, P. T. *Biochemistry* **2000**, *39*, 2552–2563.
(17) Davidson, W. S.; Jonas, A.; Clayton, D. F.; George, J. M. *J. Biol. Chem.* **1998**, *273*, 9443–9449.
(18) Eliezer, D.; Kutluay, E.; Bussell, R.; Browne, G. *J. Mol. Biol.* **2001**, *307*, 1061–1073.
(19) Bussell, R.; Eliezer, D. *J. Mol. Biol.* **2003**, *329*, 763–778.
(20) Chandra, S.; Chen, X. C.; Rizo, J.; Jahn, R.; Sudhof, T. C. *J. Biol. Chem.* **2003**, *278*, 15313–15318.

(21) Ramakrishnan, M.; Jensen, P. H.; Marsh, D. *Biochemistry* **2003**, *42*, 12919–12926.
(22) Jao, C. C.; Der-Sarkissian, A.; Chen, J.; Langen, R. *Proc. Natl. Acad. Sci. U. S. A.* **2004**, *101*, 8331–8336.
(23) Narayanan, V.; Scarlata, S. *Biochemistry* **2001**, *40*, 9927–9934.
(24) Lee, H. J.; Choi, C.; Lee, S. J. *J. Biol. Chem.* **2002**, *277*, 671–678.
(25) Volles, M. J.; Lansbury, P. T. *Biochemistry* **2002**, *41*, 4595–4602.
(26) Zhu, M.; Li, J.; Fink, A. L. *J. Biol. Chem.* **2003**, *278*, 40186–40197.
(27) Perrin, R. J.; Woods, W. S.; Clayton, D. F.; George, J. M. *J. Biol. Chem.* **2000**, *275*, 34393–34398.
(28) McLean, P. J.; Kawamata, H.; Ribich, S.; Hyman, B. T. *J. Biol. Chem.* **2000**, *275*, 8812–8816.
(29) Jo, E. J.; McLaurin, J.; Yip, C. M.; St George-Hyslop, P.; Fraser, P. E. *J. Biol. Chem.* **2000**, *275*, 34328–34334.
(30) Ueda, K.; Fukushima, H.; Masliah, E.; Xia, Y.; Iwai, A.; Yoshimoto, M.; Otero, D. A. C.; Kondo, J.; Ihara, Y.; Saitoh, T. *Proc. Natl. Acad. Sci. U. S. A.* **1993**, *90*, 11282–11286.
(31) Winkler, G. R.; Harkins, S. B.; Lee, J. C.; Gray, H. B. *J. Phys. Chem. B* **2006**, *110*, 7058–7061.
(32) Rischel, C. *J. Mol. Biol.* **1996**, *257*, 877–885.
(33) Riordan, J. F.; Vallee, B. L. *Meth. Enzymol.* **1972**, *25*, 515–521.
(34) Kim, J. E.; Arjara, G.; Richards, J. H.; Gray, H. B.; Winkler, J. R. *J. Phys. Chem. B* **2006**, *110*, 17656–17662.
(35) Wu, P. G.; Brand, L. *Anal. Biochem.* **1994**, *218*, 1–13.
(36) Reshetnyak, Y. K.; Koshevnik, Y.; Burstein, E. A. *Biophys. J.* **2001**, *81*, 1735–1758.
(37) Kleinschmidt, J. H.; den Blaauwen, T.; Driessen, A. J. M.; Tamm, L. K. *Biochemistry* **1999**, *38*, 5006–5016.
(38) Doring, K.; Konermann, L.; Surrey, T.; Jahnig, F. *Eur. Biophys. J.* **1995**, *23*, 423–432.
(39) Surrey, T.; Jahnig, F. *Proc. Natl. Acad. Sci. U. S. A.* **1992**, *89*, 7457–7461.